TISSUE ENGINEERING: Part A
Volume 21, Numbers 5 and 6, 2015

DOI: 10.1089/ten.tea.2014.0271

An *In-Situ* Forming Skin Substitute Improves Healing Outcome in a Hypertrophic Scar Model

Ryan Hartwell, BSc, Malihe-Sadat Poormasjedi-Meibod, MSc,* Claudia Chavez-Munoz, MD, PhD,*
Reza B. Jalili, MD, PhD, Azadeh Hossenini-Tabatabaei, PharmD, PhD, and Aziz Ghahary, PhD

Wound repair requires a sequential series of biological events that begins with the deposition of a temporary scaffold within which cells can repair the skin. Without a scaffold, repair is essentially impossible. Aberrant wound healing, such as hypertrophic scarring or nonhealing, has a tremendous burden on healthcare and quality of life. Timely wound closure dramatically reduces the risk of infection and scarring. Cellular skin substitutes are opportune to meet this need. Our goal was to create an *in-situ* forming scaffold that can be easily combined with cells to rapidly form a dermal substitute within the wound bed. In this study, we evaluated the application of a polyvinyl alcohol-collagen-glycosaminoglycan-based biohybrid scaffold system in full-thickness wounds on a rabbit fibrotic ear model. Punch wounds (6 mm) were either untreated or filled with an acellular scaffold, a scaffold containing xenofibroblasts, or a scaffold containing xenofibroblasts expressing indoleamine 2,3-dioxygenase (IDO). Results demonstrated that (1) both acellular and IDO-expressing fibroblast *in-situ* forming scaffolds significantly reduced scar elevation index (1.24 ± 0.05 and 1.25 ± 0.03; $p < 0.05$) and improved overall healing quality compared with xenofibroblast scaffolds and untreated wounds; (2) IDO-expressing fibroblast scaffolds significantly reduced T-cell infiltration into the scaffold-engrafted area ($p < 0.05$); and (3) both IDO-expressing and acellular *in-situ* forming scaffolds demonstrated increased vessel-like and nerve-like structures ($p < 0.05$). The results demonstrated that the use of the *in-situ* forming scaffold, and even more so when delivering IDO-expressing cells, improved healing outcome in full-thickness hypertrophic rabbit ear wounds.

Introduction

Wound healing is a complex and dynamic process, by which skin cells orchestrate cell–cell communication to repair injured tissue. Use of engineered skin substitutes is intended to foster timely and normal healing. Unfortunately, not all wounds undergo organized healing and are often stuck in a non- or over-healing phase.[1–4] Many diabetic and severe burn patients lack adequate donor sites to be used for autografts. The need for a patient ready integratable skin substitute is underscored by the roughly 20 million diabetic ulcer patients each year in North America, many of whom end up requiring amputation, and an excess of 400,000 hospitalized burn patients who desperately require a means of tissue repair.[5–7]

The medical device field has exploded with biological and tissue-engineered products for advanced wound care.[5,8–10] Some of these commercially available products include biologics and biologic hybrids such as bi-layered allografts and acellular scaffolds. As with any product, continuous development seeks to improve caveats that exist with current wound-care modalities. For example, cost and supply chain logistics have retarded the economic advancement of many advanced wound-care devices.[6,10] Second, allogeneic cellular scaffolds can elicit an immune rejection response that, although are often unpronounced, may further complicate healing.[9,11] In spite of these hurdles, the success of allo/xenogenic-tissue substitutes remains an ongoing discussion.

Many scaffolds that are currently used are preformed, solid materials. These scaffolds, including autografts, are unable to immediately integrate with the uneven surface of a wound bed. Without sufficient integration, there is a risk of graft loss.

Hydrogels can be integratable, but are often created using components such as alginates, p-HEMA, chitosan, and, in some cases, macro-sphere fillers.[12–17] The downside to many of injectable scaffolds is the poor mechanical strength in comparison to solid structures. Ideally, the interface between the scaffold and the wound bed should be seamless and, thus, promote vascular perfusion and innervation. We have previously proposed an *in-situ* forming collagen scaffold that, as an intact scaffold sheet, can serve as a hydrated skin substitute. In combination with cells, this scaffold can also serve as an easily prepared, patient-ready skin substitute for burns and chronic wounds.[18] Earlier data have demonstrated that

Department of Surgery, University of British Columbia, Vancouver, Canada.
*These authors contributed equally.

Indoleamine 2,3-dioxygenase (IDO)-expressing cells could protect xeno/allotransplants from T-cell-mediated rejection[2,19–21] but require lengthy preparation time (>2 weeks) to create a skin substitute. We have also demonstrated that a polyvinyl alcohol (PVA)-hydrogel system could be combined with a collagen-glycosaminoglycan (GAG) network to produce a rapidly gelling matrix that exhibited superior mechanical and biological properties to traditional collagen based materials *in vitro*.[18]

In this study, we present the results of a biohybrid hydrogel-collagen-GAG system that is able to rapidly transition from a viscous liquid into a solid scaffold within the wound. One primary objective of this study was to evaluate the effectiveness of this system to adequately form within the wound, in the presence of biological fluids, and integrate with surrounding tissue. Working toward the application of a patient-ready skin substitute, this study demonstrates the functionality and feasibility of an *in-situ* forming hydrogel collagen-GAG scaffold to be combined with IDO-expressing cells, thereby improving healing outcome in a hypertrophic animal model.

Materials and Methods

Cell isolation and culture

In accordance with the human ethics policy at the University of British Columbia, primary fibroblasts were isolated from the discarded foreskins of three consenting donors. Likewise, primary hypertrophic scar fibroblasts were isolated from the skin of three consenting donors (one child [<18 years] and two adults [≥18 years]) that was discarded after surgical procedures. Skin specimens were briefly washed several times with 1× phosphate-buffered saline (PBS) (pH 7), containing 1% antibiotic, minced into small pieces, and then fixated with fetal bovine serum (FBS) for 4 h on a tissue culture plate. After 6 h, one drop of 1× Dulbecco's modified essential medium (DMEM) containing 10% FBS and 1% antibiotic was added to the FBS drops overnight. The next day, DMEM was used to cover fixated skin section in the dish. Skin pieces were maintained in culture until fibroblasts reached 60% confluency, after which cells were trypsinized and passaged as per previous studies.[2,19,22] Fibroblasts in passage 6–7 were used for experimentation.

Preparation of IDO-expressing cells

Dermal fibroblasts were stably transduced to over-express IDO using a recombinant lentivirial vector constructed by our group as previously performed[2,19,22] with modifications using a blasticidin selection gene. Infected IDO-expressing cell population was then enriched through blasticidin addition (8 μg/mL) to the media after exposure and washout of live virus. IDO expression in transduced fibroblasts was confirmed through polymerase chain reaction of *hIDO* mRNA (Fig. 1A) run on a 1% agarose gel. Expression of functional IDO was confirmed by measuring kynurenine levels in the conditioned media (Supplementary Fig. S1B; Supplementary Data are available online at www.liebertpub.com/tea).

Scaffold preparation

Crosslinked collagen-GAG scaffolds were prepared as previously described.[18,23] Briefly, Type 1 bovine collagen (Advanced Biomatrix) and chondroitin-6-sulfate (Sigma

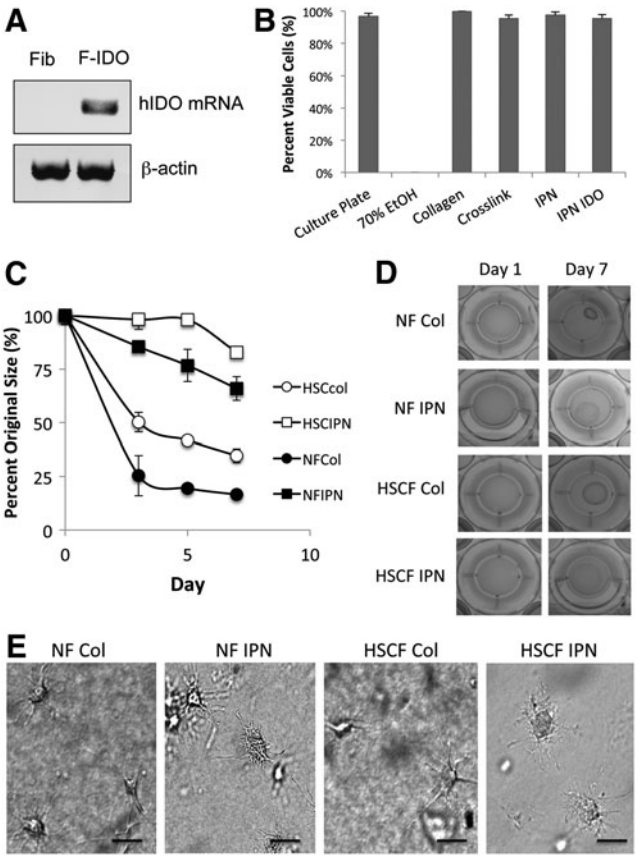

FIG. 1. Biocompatibility and functional evaluation of scaffolds *in vitro*. **(A)** Validation of hIDO expression in human fibroblasts transfected with IDO using a lentiviral vector system driven by ef1α as previously published.[21] Detection of hIDO mRNA in transduced fibroblasts (IDOF) by polymerase chain reaction. No mRNA expression of hIDO was detected in nontransfected cells (Fib). **(B)** Viability of primary fibroblasts and IDO cultured in scaffolds: collagen (collagen + GAG), crosslinked (glutaraldehyde crosslinked collagen + GAG), and IPN (glutaraldehyde crosslinked collagen + GAG + hydrogel) ($n=3$; $p>0.05$) **(C)** Graphical representation of free-floating scaffold resistance to contraction over a 7 day period. Fibroblasts derived from normal (NF) and hypertrophic scar (HSC) tissues were cultured in either standard collagen-GAG scaffolds (Col) or *in-situ* forming scaffolds (IPN) and observed for contracture over a 7-day period ($n=3$; $p<0.05$). **(D)** Photographic of representation of free-floating scaffolds. **(E)** Inverted microscopic live cell imaging of fibroblasts cultured in scaffolds after 24 h of incubation (scale bar = 50 μm). GAG, glycosaminoglycan; IDO, indoleamine 2,3-dioxygenase; IPN, interpenetrating network.

Aldrich) were combined (1:6 w/w ratio) to a final concentration of 3 mg/mL collagen and neutralized with DMEM and 1N NaOH. Glutaraldehyde (0.02% v/v; Sigma Aldrich) was used to crosslink the collagen for 1 h on ice in the dark. After crosslinking, glycine was used to de-activate residual aldehydes. After washing, hydrogels comprising PVA (50:50/208,000 and 146,000 MW, 0.2%w/v; Sigma Aldrich), sodium borate decahydrate (0.05%w/v; Sigma Aldrich), and ascorbate (pH 7, 100 μM; Sigma Aldrich) were added to the crosslinked collagen to fabricate *in-situ* forming scaffolds. All scaffolds were maintained at 4°C in liquid form until they were used for evaluation.

Cell viability and morphology

The viability of cells cultured within the scaffolds was examined using calcein AM and ethidium homodimer as previously described.[18,23] Briefly, cells within scaffolds were washed with 1× PBS, then exposed to calcein AM (1 μL/mL) and ethidium homodimer (4 μL/mL), and incubated for 30 min. After incubation, scaffolds were washed again with 1× PBS and then visualized and counted for live and dead cells using Image J (NIH software). Gray-scale, phase-contrast images of cell morphology were taken 24 h after gelation. All cell images were captured using a Zeiss Axiovert microscope and Axiovision 4.8 software.

Scaffold contracture

Human fibroblasts from normal (NF) and hypertrophic scar (HSC) tissues were cultured within either collagen scaffolds without hydrogel (Col) or *in-situ* forming scaffolds interpenetrating network (IPN) that were prepared as previously described.[18] Cell media (DMEM containing 10× FBS and 1× antibiotics) was changed daily. Fibroblast-populated scaffolds (400 μL volume with 250,000 cells/mL) were released from the plate walls at 24 h after gelation (on day 0) and allowed to float. Images were taken on release and on days 1, 3, 5, and 7 using a Sony digital camera at a consistent range. Scaffold size was measured using Image J (NIH software).

Animal model

All animal models were employed in accordance with protocols approved by the University of British Columbia and the Canadian Guidelines on Animal Care. Aseptic surgical techniques were used for all procedures. As a standard model of scar hypertrophy, four New Zealand white rabbits (~3 kg) were used to investigate the utility of the *in-situ* forming scaffolds to be employed as skin substitutes as previously published.[2,24–26] Animals were anesthetized using ketamine/xylazine induction and isoflourene maintenance. Meloxicam (0.3 mg/Kg) prophylaxis was used as an analgesic. Four 6 mm full-thickness punch wounds were created on the dorsal surface of both ears and randomized by location. Groups and wound numbers were as follows:[8] untreated control (Con);[8] acellular *in-situ* forming scaffolds (Gel);[8] *in-situ* forming scaffolds containing normal human fibroblasts (GelF); and[8] *in-situ* forming scaffolds containing normal human IDO-expressing fibroblasts (Gel IDOF). Cells were combined with scaffolds (pregelation) at a concentration of 500,000 cells/mL. Scaffolds were maintained in a liquid form on ice before creation of the wounds. Once wounds were formed, gels were aspirated within a 16G catheter and warmed for 5 min on a heating blanket before injecting onto the wound. Wounds were covered using Steri-Strips (3M Healthcare) and Tegaderm™ (3M Healthcare) occlusive dressing. Rabbits were inoculated with additional *in-situ* forming scaffolds (once daily) for 4 days after wounding using a 16G catheter to overcome thinning of the scaffold that occurred after gelation. The catheter was placed within the Tegaderm dressing and subsequently closed thereafter on covering. Rabbits were evaluated over a 35-day period to assess scarring and healing outcomes.

Healing outcome - scar elevation index, epidermal thickness, and cellularity

Quality of wound healing can be measured in a number of ways, three of which are the scar elevation index (SEI), epidermal thickness (ET), and cellularity.[2,24–26] The SEI can easily be calculated using a formula (1) and it is a measure of the ratio in ET and dermal thickness (DT) of the wounded area to that of the adjacent normal skin. DT and ET are secondary markers of scarring and are calculated as the average pixel thickness across the neo-tissue. Thickened dermis and/or epidermis are often observed in HSC and keloids, with a marked abundance of collagen deposition. Healing rate was assessed qualitatively on day 20, once wounds had begun to epithelialize. Increased cellularity is a hallmark indicator of fibroproliferative disorders such as hypertrophy, especially in its early stages, and is easily quantified as cells/high-powered field (hpf) using Image J (NIH software).

$$\text{SEI} = \text{Cross-Sectional Area of Healed Dermis} / \text{Original Cross-Sectional Dermal Area} \quad (1)$$

Collagen staining, matrix metalloproteinase-1, and collagen expression

To determine the abundance of collagen deposition, paraffin-embedded sections were de-waxed and stained for collagen with Masson's Trichrome as previously described.[25] Keratin and muscle fibers are stained red, collagen fibers are stained blue, and cell cytoplasm and nuclei are stained light pink and dark brown. Total RNA was extracted from scar tissue using Trizol reagent according to the manufacturer's instructions (Invitrogen). After DNase treatment and cDNA synthesis, gene expression of matrix metalloproteinase-1 (MMP1) and pro-alpha-1-collagen (col1a1) was determined using q-PCR (AB Biosystems). Primers, described in Table 1, were designed and purchased from Invitrogen. β-actin was used as the reference gene.

Immunofluorescent staining of CD31, CD3, and PGP 9.5

Tissues were fixed in 10% formalin at room temperature and then embedded in paraffin followed by sectioning into 5 μm sections. Embedded sections were then stained using both immunohistochemical and immunfluorescent techniques. Antigen retrieval was carried out in sodium citrate buffer (pH 6.0). Tissue was first incubated with blocking buffer (5% Goat Serum/5% Albumin in 1× PBS [pH 7]) for 1 and for 2 h with anti-CD3 (using 5% horse serum) at room temperature. Tissue sections were then incubated with

Table 1. Polymerase Chain Reaction Primer Sequences

Gene	*Sequence (F/R)*
Col-α1	GGACCTCAAGATGTGCCACT/ ACCACACGTGCTTCTTCTCC
MMP1	CAGCTTTATGGGAGCCAGTC/ TGTTCCTCACCCTCCAGAAC
hIDO	GGCAAAGGTCATGGAGATGT/ CTGCAGTCTCCATCACGAAA

primary anti-bodies CD31 (1:50; Santa Cruz), CD3 (1:50), and PGP 9.5 (1:25; Abcam, Inc.) overnight at 4°C. All sections were incubated with secondary antibody at room temperature (Alexa-fluor 488 anti-rabbit 1:2000, Alexa-fluor 568 anti-goat 1:1000; Invitrogen). 4′-6-Diamidino-2-phenylindole (DAPI; Vector Laboratories, Inc.) was used as a counter stain. Sections were viewed using a Zeiss Axiovert microscope and Axiovision 4.8 software. Image analysis was conducted using Image J (NIH software).

Statistics

All histological and *in vitro* experiments were performed in triplicate ($n=3$). Wound analysis consisted of eight wounds per group ($n=8$), with the exception of the mRNA analysis ($n=4$). One-way analysis of variance with Tukey *post-hoc* analysis was employed to determine statistical significance. Standard deviation is represented in graphs and tables, and significance is indicated with an asterisk with an alpha of 0.05.

Results

IDO expression, skin cell viability, and morphology within in-situ *forming scaffolds*

Validation of IDO expression and activity was confirmed through detection of hIDO mRNA in transfected fibroblasts (Fig. 1A) in conjunction with measurement of increasing concentrations of kynurenine in the culture media (Supplementary Fig. S1B). Primary human fibroblasts cultured on both plastic and in the *in-situ* forming scaffolds were examined for viability 24 h after gelation. Using calcein AM and ethidium homodimer as makers of viability, it was found that cells remained similarly viable in all systems as previously found[18,23] (Fig. 1B).

Free-floating scaffold resistance to contraction and cellular morphology

Fibroblast-populated free floating scaffolds (500,000 cells/mL) were created using the *in-situ* forming scaffolds and a standard collagen-GAG scaffold similar formulation to our previous study.[18] Four different scaffolds were fabricated to examine the efficacy of scaffolds to resist contraction of NF and HSC fibroblasts. Standard collagen-GAG scaffolds containing normal fibroblasts (NFCol) attained near maximum contraction (16% of original size) within the first 3 days (Fig. 1C, D), unlike the *in-situ* forming scaffolds (NFIPN) that resisted contraction (within 85–98% of the original size) within the same period of time. As expected, all scaffolds contracted over the 7-day period, notwithstanding that the standard collagen-GAG scaffolds achieved an apparent plateau in contraction either on or nearest to the third day. *In-situ* forming scaffolds significantly resisted contraction over the 7 days compared with corresponding standard collagen-GAG scaffolds ($82.8\% \pm 0.01\%$ vs. $34.6\% \pm 3.19\%$ and $66\% \pm 11.4\%$ vs. $16\% \pm 0.01\%$ of the original size, respectively). Interestingly, normal fibroblasts were more contractive than fibroblasts derived from HSC ($16\% \pm 0.01\%$ vs. $32\% \pm 3.19\%$ of the original size) by which the initial contraction by these cells was found to be the greatest within the first 3 days. Cell morphology of cultured fibroblasts before scaffold release demonstrated cell spreading and attachment in both scaffolds with a marked reduction in refraction and an apparent difference in the morphology of cell extensions (Fig. 1E).

Application of the hydrogel scaffold and wound-healing outcome

Treated wounds received treatment with the *in-situ* forming hydrogel collagen-GAG scaffold and covered with Tegaderm as shown in Figure 2A. All wounds healed within the 35-day investigational period. Scaffolds containing xenofibroblasts (GelF) and untreated wounds were among the final wounds to heal (Fig. 2B). Wounds treated with either acellular *in-situ* forming scaffolds (Gel) or with *in-situ* forming scaffolds containing IDO-expressing fibroblasts (Gel IDOF) exhibited earlier epithelialization and minimal

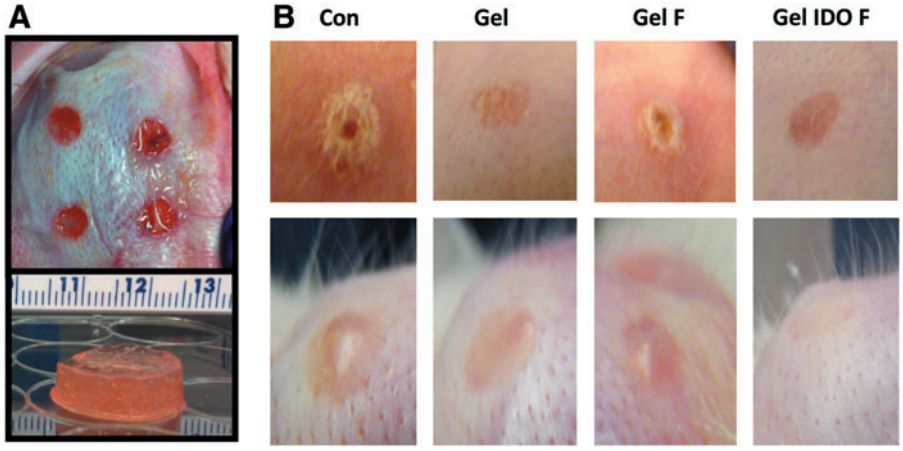

FIG. 2. Macroscopic clinical evaluation of punch wounds in the rabbit ear. **(A)** *Upper panel*: Photomicrograph depicting postsurgical punch wounds filled with a layer of *in-situ* scaffolds (*right side*) and covered with Tegaderm™ after solidification. *Lower panel*: Free-standing *in-situ* forming scaffolds after gelation in a culture dish at 37°C for 15 min. **(B)** Follow-up micrographs on postsurgical day 20 (*upper panel*) and day 35 (*lower panel*) demonstrating wound-healing progression. Con, untreated wounds; Gel, acellular *in-situ* forming hydrogel collagen-GAG scaffold; GelF, *in-situ* forming scaffolds containing xenofibroblasts; Gel IDOF, *in-situ* forming scaffolds containing IDO-expressing fibroblasts. Color images available online at www.liebertpub.com/tea

erythema on the margins. Untreated and GelF-treated wounds presented a scab and raised scar or cyst-like structure that was evident on day 20, which further resulted in a thick-to-the-touch, raised scar on day 35 of the study. All Gel or Gel IDOF-treated wounds had completed healing (free of scab) by day 20 without the formation of a raised scar or cyst-like structure (Fig. 2B).

Histological hallmarks of HSC are a thickened epithelium, rete ridges in the epidermis, dense collagen bundle formations in the dermis, low levels of MMP-1, increased and disorganized collagen type I deposition, and increased cellularity.[2,24] Figure 3A–D depicts a thickened epidermis and dermis in the untreated and GelF-treated wounds compared with normal skin and that of either Gel or Gel IDOF groups. Using the SEI, ET, and DT analysis, it was found that the application of Gel significantly reduces scarring in general compared with that of untreated and GelF-treated wounds, respectively, even in the presence of an occlusive dressing (Figs. 3A–D and 4A, B). The thickness of both epidermis and dermis was significantly lower in Gel (9.48 ± 1.83 and 0.93 ± 0.15 pixels) and Gel IDOF (9.93 ± 2.60 and 0.67 ± 0.25 pixels) groups relative to untreated wounds (17.23 ± 2.6 and 1.61 ± 0.15 pixels) (Fig. 2A, B). Furthermore, Gel and Gel IDOF treated wounds resulted in relatively similar SEI (1.24 ± 0.05 and 1.25 ± 0.03). Interestingly, ET and DT were relatively similar among Gel and Gel IDOF-treated wounds (Fig. 4A). Cellularity was also significantly lower in the Gel and Gel IDOF groups (124 ± 21 and 114 ± 17 cells/hpf), and greatest in the control group (242 ± 25 cells/hpf). Collagen bundle formations were absent in all Gel and Gel IDOF groups, and markedly higher in untreated wounds (Fig. 3). GelF group displayed collagen bundle formation but to a lesser extent than untreated wounds. Rete ridges were notable in both untreated and GelF groups (Fig. 3E–L).

Matrix deposition and expression of MMP-1 and collagen type 1

Collagen deposition was evaluated using Masson's trichrome staining (Fig. 5A). As expected, the raised scar structures of the untreated and GelF groups corresponded with a greater amount of disorganized collagen deposition. Gel and Gel IDOF-treated wounds demonstrated predominantly a parallel matrix organization that was contiguous with neighboring unwounded tissue. At the mRNA level, untreated wounds expressed increased tissue levels of pro-alpha-1 collagen and low levels of MMP-1 (25.30 ± 3.22 and 3.53 ± 0.73-fold, respectively), the primary collagen-remodeling enzyme (Fig. 5B, C). Wounds treated with Gel and Gel IDOF exhibited a significantly lower amount of tissue pro-alpha-1 collagen expression (9.57 ± 3.1 and 10.23 ± 1.95-fold, respectively; $p < 0.05$) compared with all other treatments on day 35 postwounding. When compared with the untreated group, Gel treated wounds alone did not significantly alter the MMP-1 expression (1.28 ± 0.6 vs. 0.58 ± 0.21-fold); however, Gel IDOF-treated wounds

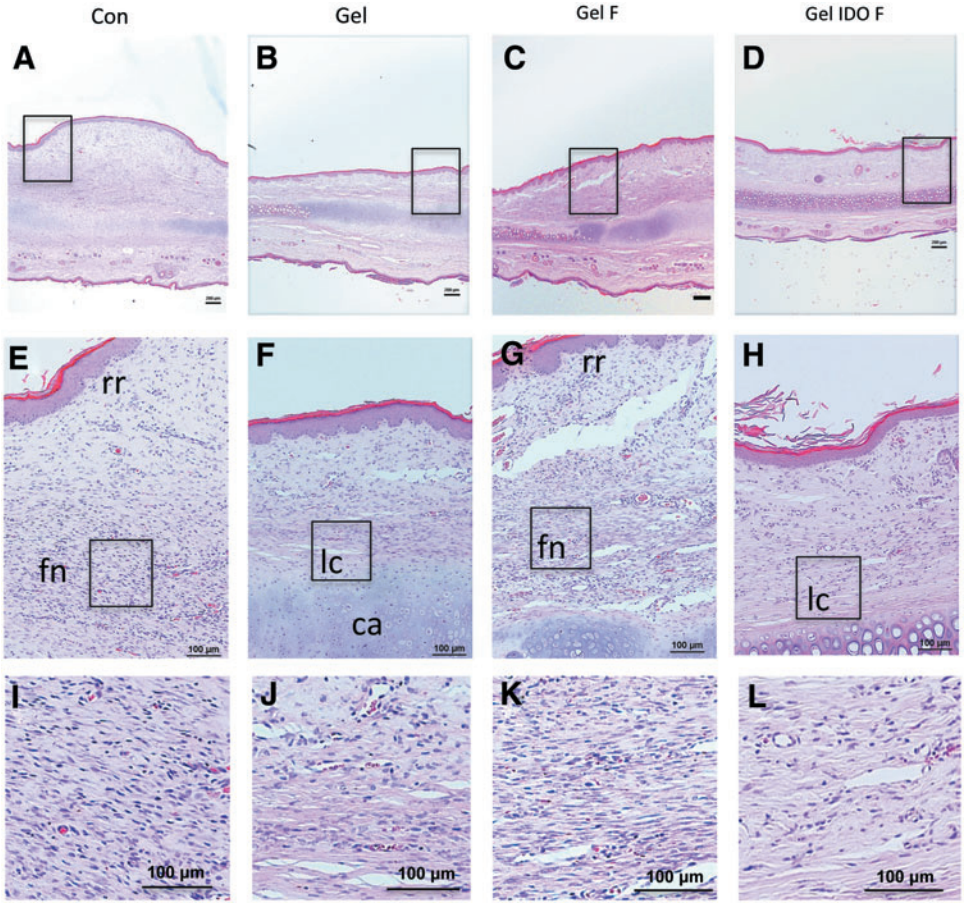

FIG. 3. **(A–L)** Histologic evaluation of hematoxylin and eosin-stained sections of treated rabbit wounds on postsurgical day 35. Abbreviations in **(E–H)** denote histological features: lc, linear collagen banding; ca, cartilage (mature and immature); fn, fibrotic nodules; rr, rete ridges. Scale bars represent 200 µm for **(A–D)** and 100 µm for **(E–L)**. *Black boxes* indicate the region represented in the corresponding *lower panel* higher magnification image. Color images available online at www.liebertpub.com/tea

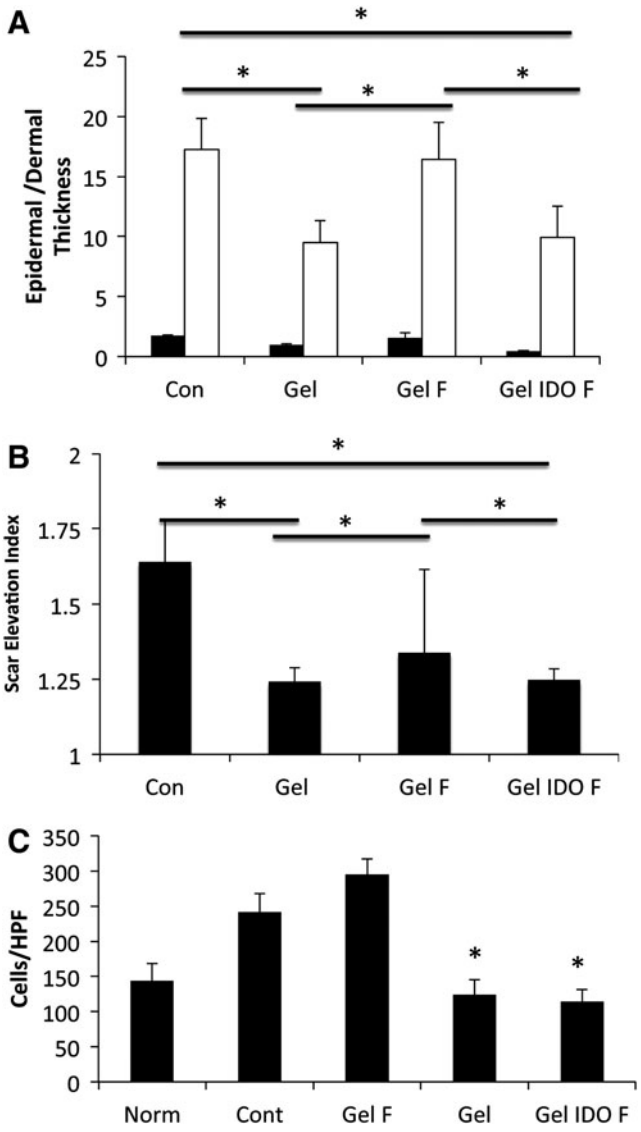

FIG. 4. Evaluation of healing outcome in rabbit ear-treated wounds using scar elevation index, epidermal and dermal thickness, and tissue cellularity. **(A)** Epidermal (*open bars*) and dermal (*closed bars*) thickness averages. Dermal thickness area scaled at 1:100,000 pixels and epidermal thickness as linear pixel averages of the treated wound area. **(B)** Scar elevation index, represented as the ratio of the total hypertrophic tissue relative to the normal tissue area. **(C)** Cellularity of hematoxylin and eosin (H&E) stained tissue sections ($n = 8$; $^*p < 0.05$).

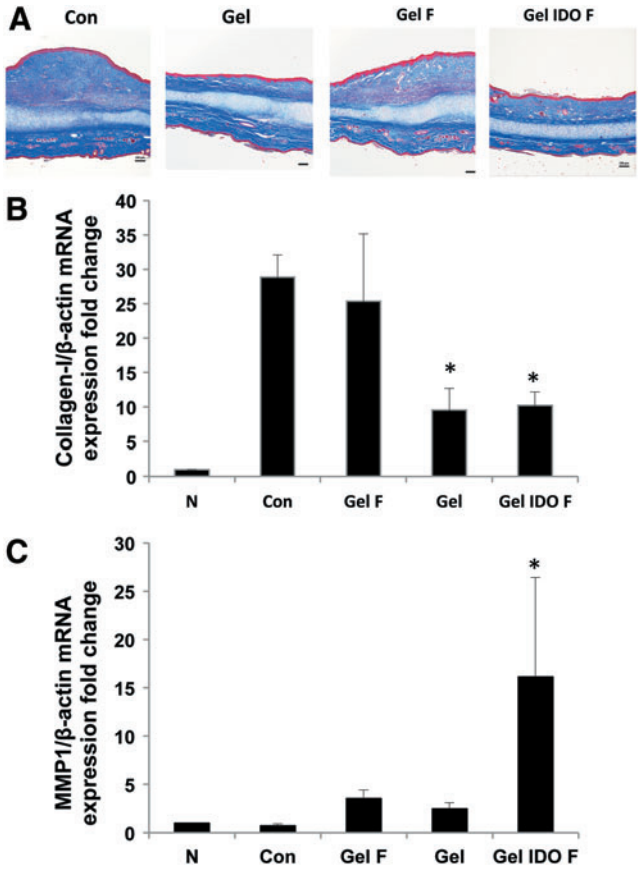

FIG. 5. Collagen staining and gene expression of collagen and MMP-1 in treated rabbit wounds. **(A)** Masson-trichrome staining of collagen in wounded tissue sections on day 35. Scale bar represents 400 μm, respectively. **(B)** mRNA expression of pro-alpha 1 Collagen in treated rabbit ear tissue. **(C)** mRNA expression of MMP-1 in treated rabbit ear tissue. All mRNA expression is expressed as a fold change in beta-actin and normalized to uninjured tissue. β-actin was used as a reference gene ($n = 8$; $^*p < 0.05$). MMP-1, matrix metalloproteinase-1. Color images available online at www.liebertpub.com/tea

exhibited a significant 16-fold increase in tissue MMP-1 expression when compared with normal skin and all other treatments. Reduced expression of pro-alpha-1-collagen in the Gel treatment group corresponded with a decreased collagen type I deposition within the wound site and the absence of scarring.

$CD3^+$ T-cells postwound healing

It is well known that localized IDO activity can prevent T-lymphocyte infiltration and proliferation.[2,19,20] T-cell infiltration and persistence in healed wounds was evaluated by immunofluorescent staining using a rabbit monoclonal anti-$CD3^+$ pan T-cell marker. Gel IDOF-treated wounds demonstrated significantly reduced, if not entirely absent, infiltrated immune cells evaluated on day 35 compared with both untreated and GelF-treated wounds (4 ± 2 vs. 8 ± 3 and 14 ± 4 cells/hpf respectively; Fig. 6A, C). Likewise, wounds treated with Gel alone exhibited relatively fewer $CD3^+$ cells on day 35 compared with the untreated wounds; however, this difference was not significant (8 ± 3 vs. 5 ± 2, $p > 0.05$). GelF-treated wounds were heavily infiltrated with $CD3^+$ cells; this may explain the increased cellularity found in these samples (Fig. 3D–L), and the number of these cells was significantly greater than the untreated wounds. Functional IDO expression was confirmed through kynurenine production within the Gel IDOF scaffold cultured *in vitro*. Gel IDOF scaffolds sustained IDO production throughout the experiment (Supplementary Fig. S1A) and were able to produce sufficient Kynurenine concentrations (15–20 μg/mL) (Supplementary Fig. S1B), as per previous studies in this range.[2,19]

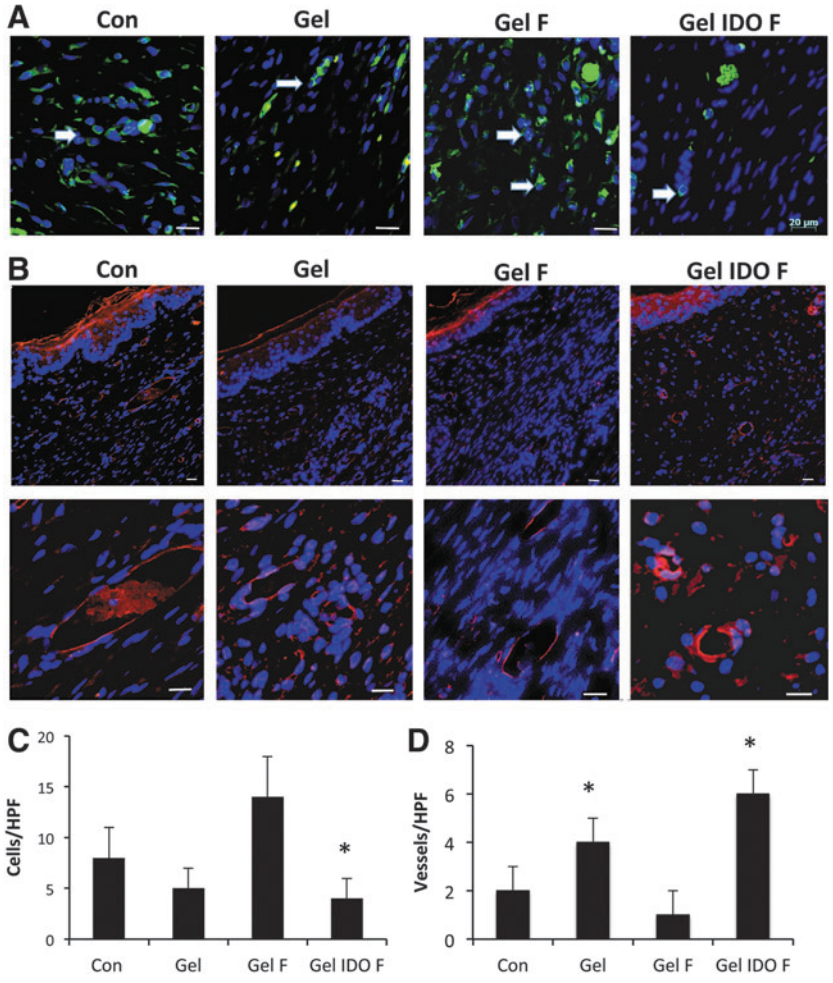

FIG. 6. $CD3^+$ lymphocyte and $CD31^+$ marked vessel formation in treated rabbit tissue. **(A, C)** Photomicrographs and corresponding quantification of $CD3^+$ lymphocyte infiltration into the wounded area represented as the number of cells per high-powered field as denoted by *white arrows* ($n=8$). **(B, D)** Photomicrographs and corresponding quantification of vessel formation within the treated wounds. ($n=8$; $*p<0.05$) (scale bars represent 50 μm).

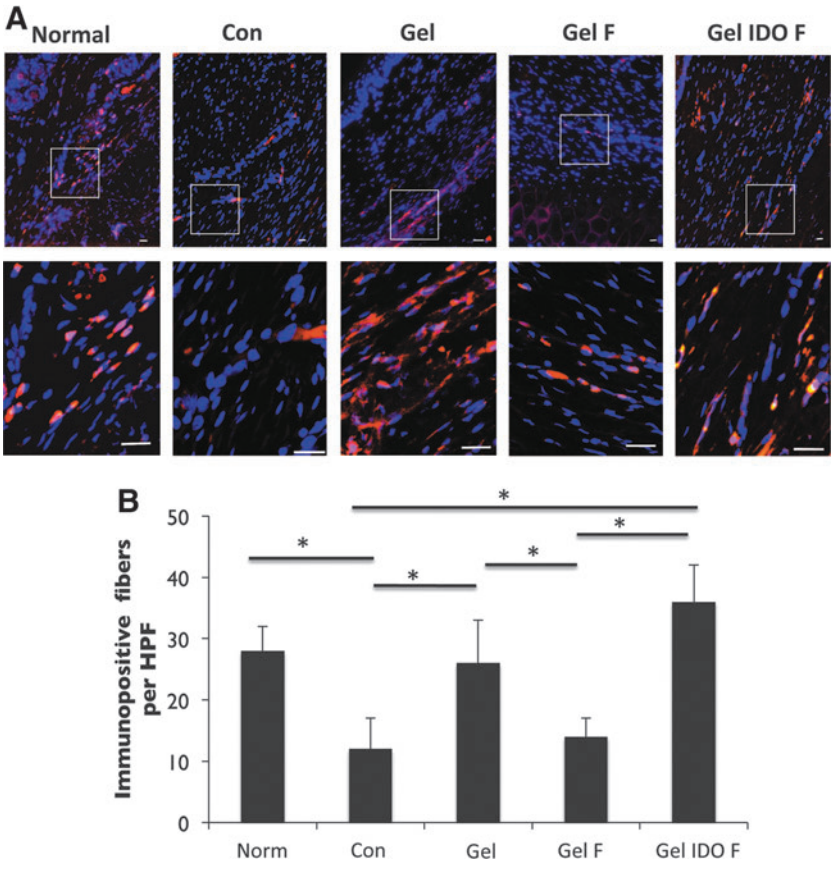

FIG. 7. Distribution and quantification of cutaneous neoinnervation within the treated wound tissues at 35 days post-surgery. **(A)** Photomicrograph representation of panaxonal marker PGP 9.5 (*red*) in tissue sections displays peripheral nerve fiber formation. *White boxes* correspond to the *lower panel* images representing staining specificity. **(B)** Quantification of fiber density is represented by number of immunopositive fibers per high-powered field ($n=8$, $*p<0.05$). Scale bar = 100 μm.

PECAM-1 immunostaining and vessel-like structures within healed wounds

Perfusion of a tissue or graft through angiogenesis is essential for oxygenation and nutrient flow.[27,28] Vessel formation was identified with immunofluorescent staining of CD31 (a specific endothelial cell marker) and confirmed both cellular organization and structure (Fig. 6B). The CD31 and vessel architecture was significantly higher in the Gel and Gel IDOF treatment groups compared with the other treatments (4 ± 1 and 6 ± 1 vessels, respectively, per hpf, $p < 0.05$; Fig. 6D).

Cutaneous innervation

Rabbit tissue from day 35 was stained for PGP 9.5 (ubiquitin hydrolase), a panaxonal marker for ganglia and nerve sheath development and a standard marker for intra-epidermal nerve fibers, including Langherans cells.[29] All wounds treated with the Gel exhibited structural formation of innervated fiber-like structures within the neo-dermis (Fig. 7A, B). This was matched with both appendages and vascular structures that typically are associated with innervated structures. Gel and Gel IDOF-treated wounds demonstrated significantly more innervation (26 ± 6 and 36 ± 6 immunoreactive fibers [IRF]/hpf) than other treatments (Con 12 ± 5 and GelF 14 ± 3 IRF/hpf) and resembled that of normal skin (28 ± 4 IRF/hpf). Gel alone was found to have a greater number of innervated structures than the GelF-treated wounds and more closely reflects un-wounded skin.

Discussion

Wound healing requires a lengthy orchestrated sequence of biological events, and any deviation in this process results in either over-healing or lack thereof. In this study, we sought improved wound-healing outcomes by the application of a novel hydrogel-collagen scaffold that can be used to fabricate a skin substitute *in situ* and integrate with all aspects of the wound bed. In principle, this solution seeks to also circumvent several issues with current solid scaffolds and engineered skin substitutes.[6,8–10,30] It is well known that timely biological wound coverage has a direct impact on healing outcome. Wounds that remain open for greater than 21 days are likely to result in hypertrophy and excessive scarring, in addition to becoming susceptible to infection, water and heat loss.[1,6,31] In our previous work, we have demonstrated the benefit of using an IDO-expressing fibroblast as an allo/xeno-transplant that will be tolerated by the recipient.[2,19,32] In this study, we constructed a skin substitute *in situ*, with and without IDO-expressing fibroblasts, that conferred greater feasibility for clinical application over previous works. Through the combination of a partially crosslinked hydrogel-collagen biohybrid system, we are able to rapidly decrease the gelation time of the scaffold. Consistent with our previous work, the addition of a PVA hydrogel to the collagen network lends itself to produce a tacky rapidly forming scaffold that is easily applied to the wound bed without compromising cell viability (Fig. 2B).[18,23] It was previously demonstrated that PVA-hydrogel addition to the collagen composite produces a tacky scaffold, improves the gelation rate and mechanical stiffness[18] similar to chondroitin-6-sulfate.[33] which we found to be optimal for surgical application. The utility of this hydrogel blend is currently being explored to understand the molecular interactions that are provisional for the rapid gelation of the bio-hybrid system. Unlike other animals, rabbit ear skin heals through secondary intention (similar to humans), as opposed to contracture, and if the dermis is not replaced, hypertrophy occurs. Application of the Gel alone significantly reduced scar formation, resulting in a neodermis within which adjacent cells could infiltrate. To fabricate a patient-ready skin substitute, we investigated the application of the *in-situ* forming scaffold comprising IDO-expressing fibroblasts. The utility of the scaffold as a cell delivery vehicle markedly reduced the days required for the fabrication of a fibroblast-populated scaffold (typically 7–14 days) using preformed solid scaffolds.[2] Gel IDOF further improved the healing outcome through a reduction in SEI, ET, DT, and cellularity when compared with GelF and untreated wounds. Notably, the acellular *in-situ* forming hydrogel collagen-GAG scaffolds also provided significant improvements to wound-healing outcomes. Although acellular *in-situ* forming scaffold is advantageous for the smaller acute wounds, the additional growth factor and immunomodulatory support from IDO-expressing fibroblasts is opportune to improve healing outcomes of the nonhealing wounds or large burn wounds.[1,6,34]

IDO-expressing fibroblasts were easily combined with the *in-situ* forming scaffold in the surgical suite before applying it to the wound. As expected, GelF elicited an inflammatory response, which likely further exacerbated the fibroproliferative response despite the presence of the *in-situ* forming hydrogel collagen-GAG scaffold. Importantly, our results here correspond with previous studies demonstrating the efficacy of IDO to protect allo/xenogenic grafts and reduce scarring.[2,19,32] Earlier studies on the *in-situ* forming scaffold identified that cells cultured within the scaffolds would align in a parallel arrangement, possibly in line with fibers.[18] The defined cellular organization did not occur throughout the entirety of treated wounds, but was prominent in the hypodermis and mid-dermal sections closest to the cartilage (Fig. 3E–H). Two reasons for the lack of cellular alignment throughout the dermis could be that (1) during remodeling cells will alter the architecture of the dermis, or (2) that the scaffold is reduced to a thinner layer that is subsequently covered with an endogenous neodermis. Although GelF became hypertrophic, as expected, the extent of the hypertrophy appeared less than in our previous work using solid, premade skin substitutes.[2] It is possible that because the number of transplanted cells, including the lack of highly antigenic keratinocytes, is less than what was previously employed, the immune response is also reduced. This improved reduction in the infiltrated immune cell response would be similar to what we have observed through the use of the graft in islet transplantation models.[32]

Surgical engraftment of engineered skin and even acellular scaffolds is often burdened by the lack of vasculature in the graft and in the later stages, a restorative lack of functional innervation. For many patients, the lack of innervation within a graft site leads to idiopathic hypersensitivity and itchiness.[35] It has been reported that neovascularization, which is only suggestive of a perfused tissue, can occur as early as 14 days after engraftment in humans.[27,28] The application of a thin layer-by-layer scaffold may minimize

hypoxia, which has previously been shown to be detrimental for tissue reconstruction.[28] As was previously demonstrated, IDO expression exhibited increased mature vessel formation compared with untreated and non-IDO-expressing fibroblast engraftment.[19,36] Similarly, it was found that both Gel alone and Gel IDOF-treated wounds exhibited a greater abundance of immunoreactive nerve fibers within the hypodermis. It is unclear what type of peripheral nerve fiber has resulted and whether or not a functional nerve network will result; however, the distribution of the fibers suggests that the outcome is similar to normal tissue. Further work is warranted to investigate neovascularization within early time points, modeling vascular perfusion, and long-term nerve functionality.

Typically grafted wounds will exhibit contracture at the margins.[3] To correlate our *in vivo* findings to human tissue, scaffolds containing both human scar-derived fibroblasts and normal fibroblasts were evaluated for contractility. Results demonstrated that our *in-situ* forming scaffold could withstand the contractile tendency of normal and hypertrophic fibroblast. Although it is known that fibroblasts from HSC exhibit different phenotypic characteristics than normal cells, it was not expected that within the free-floating scaffolds they would exhibit reduced contraction when compared with normal, neonatal foreskin fibroblasts. It is well known that fibroblasts from young patients exhibit a more proliferative and active cell type (fetal being the most active), which may, in part, explain why we observed greater contractility when using neonatal fibroblasts.[37]

Conclusion

This study demonstrates for the first time the application of a nonrejectable, *in situ* forming scaffold for skin engineering. Our approach offers a promising practice to reduce the logistical and physiological hurdles that are associated with current modalities. The findings here underscore the advantages and utility of our *in-situ* gelling scaffold to be used in conjunction with nonrejectable, IDO-expressing cells to create a patient-ready skin substitute at the bedside.

Acknowledgments

This study was supported by the Canadian Institute of Health Research (CIHR), National Sciences and Engineering Research Council (NSERC), and the International Brotherhood of Electrical Workers. Ryan Hartwell holds a CIHR-SRTC doctoral graduate research award. Dr. C. Chavez-Munoz holds a CIHR-doctoral graduate award and Michael Smith Foundation for Health Research (MSFHR) Junior award. The authors thank Dr. A.M. Rezakhanloo for providing the lentiviral vector and Dr. Ruhi Kilani for her assistance in the preparation of this article.

Disclosure Statement

No competing financial interests exist.

References

1. Medina, A., Scott, P.G., Ghahary, A., and Tredget, E.E. Pathophysiology of chronic nonhealing wounds. J Burn Care Rehabil **26,** 306, 2005.
2. Chavez-Munoz, C., Hartwell, R., Jalili, R.B., Carr, M., Kilani, R.T., Jafarnejad, S.M., *et al.* Application of an indoleamine 2,3-dioxygenase-expressing skin substitute improves scar formation in a fibrotic animal model. J Invest Dermatol **132,** 1501, 2012.
3. Curran, T.A., and Ghahary, A. Evidence of a role for fibrocyte and keratinocyte-like cells in the formation of hypertrophic scars. J Burn Care Res **34,** 227, 2013.
4. Ghahary, A., Karami-Busheri, F., Marcoux, Y., Li, Y., Tredget, E.E., Kilani, R.T., *et al.* Keratinocyte-releasable stratifin functions as a potent collagenase-stimulating factor in fibroblasts. J Invest Dermatol **122,** 1188, 2004.
5. Crandall, M.A. ''Wound care Markets 2012'' Kalorama Information (2012). Publication. New York, 2010.
6. Clark, R.A., Ghosh, K., and Tonnesen, M.G. Tissue engineering for cutaneous wounds. J Invest Dermatol **127,** 1018, 2007.
7. Burn Incidence Fact Sheet [Electronic]. American Burn Association; 2014 [updated 2013; cited 2014 August 2014]. Available from: www.ameriburn.org/resources_factsheet.php
8. US Tissue Engineering Markets: Overview, Analysis and Opportunities. Frost & Sullivan, 2012, Contract No.: N910-54.
9. FDA. Technology Assessment: Skin Substitutes for Treating Chronic Wounds. FDA Publication Agency for Healthcare, 2011.
10. UILO. Skin Tissue Engineering. Vancouver: University of British Columbia, 2012. Report No.: HLC101A_S003.
11. Zaulyanov, L., and Kirsner, R.S. A review of a bi-layered living cell treatment (Apligraf) in the treatment of venous leg ulcers and diabetic foot ulcers. Clin Interv Aging **2,** 93, 2007.
12. Yildirimer, L., Thanh, N.T., and Seifalian, A.M. Skin regeneration scaffolds: a multimodal bottom-up approach. Trends Biotechnol **30,** 638, 2012.
13. Krebs, M.D., Sutter, K.A., Lin, A.S., Guldberg, R.E., and Alsberg, E. Injectable poly(lactic-co-glycolic) acid scaffolds with *in situ* pore formation for tissue engineering. Acta Biomater **5,** 2847, 2009.
14. Lu, G., Ling, K., Zhao, P., Xu, Z., Deng, C., Zheng, H., *et al.* A novel *in situ*-formed hydrogel wound dressing by the photocross-linking of a chitosan derivative. Wound Repair Regen **18,** 70, 2010.
15. Wang, L., and Stegemann, J.P. Thermogelling chitosan and collagen composite hydrogels initiated with beta-glycerophosphate for bone tissue engineering. Biomaterials **31,** 3976, 2010.
16. Meng, X., Stout, D.A., Sun, L., Beingessner, R.L., Fenniri, H., and Webster, T.J. Novel injectable biomimetic hydrogels with carbon nanofibers and self assembled rosette nanotubes for myocardial applications. J Biomed Mater Res Part A **101,** 1095, 2013.
17. Gao, L., Gan, H., Meng, Z., Gu, R., Wu, Z., Zhang, L., *et al.* Effects of genipin cross-linking of chitosan hydrogels on cellular adhesion and viability. Colloids Surf B Biointerfaces **117,** 398, 2014.
18. Hartwell, R., Leung, V., Chavez-Munoz, C., Nabai, L., Yang, H., Ko, F., *et al.* A novel hydrogel-collagen composite improves functionality of an injectable extracellular matrix. Acta Biomater **7,** 3060, 2011.
19. Forouzandeh, F., Jalili, R.B., Hartwell, R.V., Allan, S.E., Boyce, S., Supp, D., *et al.* Local expression of indoleamine 2,3-dioxygenase suppresses T-cell-mediated rejection of an engineered bilayer skin substitute. Wound Repair Regen **18,** 614, 2010.

20. Forouzandeh, F., Jalili, R.B., Germain, M., Duronio, V., and Ghahary, A. Skin cells, but not T cells, are resistant to indoleamine 2, 3-dioxygenase (IDO) expressed by allogeneic fibroblasts. Wound Repair Regen **16,** 379, 2008.
21. Elmaagacli, A.H., Ditschkowski, M., Steckel, N.K., Gromke, T., Ottinger, H., Hillen, U., *et al.* Human chorionic gonadotropin and indolamine 2,3-dioxygenase in patients with GVHD. Bone Marrow Transplant **49,** 800, 2014.
22. Rezakhanlou, A.M., Habibi, D., Lai, A., Jalili, R.B., Ong, C.J., and Ghahary, A. Highly efficient stable expression of indoleamine 2,3 dioxygenase gene in primary fibroblasts. Biol Proced Online **12,** 107, 2010.
23. Hosseini-Tabatabaei, A., Jalili, R.B., Hartwell, R., Salimi, S., Kilani, R.T., and Ghahary, A. Embedding islet in a liquid scaffold increases islet viability and function. Can J Diabetes **37,** 27, 2013.
24. Kloeters, O., Tandara, A., and Mustoe, T.A. Hypertrophic scar model in the rabbit ear: a reproducible model for studying scar tissue behavior with new observations on silicone gel sheeting for scar reduction. Wound Repair Regen **15 Suppl 1,** S40, 2007.
25. Rahmani-Neishaboor, E., Jallili, R., Hartwell, R., Leung, V., Carr, N., and Ghahary, A. Topical application of a film-forming emulgel dressing that controls the release of stratifin and acetylsalicylic acid and improves/prevents hypertrophic scarring. Wound Repair Regen **21,** 55, 2013.
26. Li, Y., Kilani, R.T., Rahmani-Neishaboor, E., Jalili, R.B., and Ghahary, A. Kynurenine increases matrix metalloproteinase-1 and -3 expression in cultured dermal fibroblasts and improves scarring *in vivo*. J Invest Dermatol **134,** 643, 2014.
27. Kung, E.F., Wang, F., and Schechner, J.S. *In vivo* perfusion of human skin substitutes with microvessels formed by adult circulating endothelial progenitor cells. Dermatol Surg **34,** 137, 2008.
28. Auger, F.A., Gibot, L., and Lacroix, D. The pivotal role of vascularization in tissue engineering. Annu Rev Biomed Eng **15,** 177, 2013.
29. Wallengren, J., Chen, D., and Sundler, F. Neuropeptide-containing C-fibres and wound healing in rat skin. Neither capsaicin nor peripheral neurotomy affect the rate of healing. Br J Dermatol **140,** 400, 1999.
30. Prestwich, G.D. Engineering a clinically-useful matrix for cell therapy. Organogenesis **4,** 42, 2008.
31. Deitch, E.A., Wheelahan, T.M., Rose, M.P., Clothier, J., and Cotter, J. Hypertrophic burn scars: analysis of variables. J Trauma **23,** 895, 1983.
32. Jalili, R.B., Forouzandeh, F., Rezakhanlou, A.M., Hartwell, R., Medina, A., Warnock, G.L., *et al.* Local expression of indoleamine 2,3 dioxygenase in syngeneic fibroblasts significantly prolongs survival of an engineered three-dimensional islet allograft. Diabetes **59,** 2219, 2010.
33. Kinneberg, K.R., Nirmalanandhan, V.S., Juncosa-Melvin, N., Powell, H.M., Boyce, S.T., Shearn, J.T., *et al.* Chondroitin-6-sulfate incorporation and mechanical stimulation increase MSC-collagen sponge construct stiffness. J Orthop Res **28,** 1092, 2010.
34. Werner, S., Krieg, T., and Smola, H. Keratinocyte-fibroblast interactions in wound healing. J Invest Dermatol **127,** 998, 2007.
35. Cheng, B., Liu, H.W., and Fu, X.B. Update on pruritic mechanisms of hypertrophic scars in postburn patients: the potential role of opioids and their receptors. J Burn Care Res **32,** e118, 2011.
36. Li, Y., Tredget, E.E., Ghaffari, A., Lin, X., Kilani, R.T., and Ghahary, A. Local expression of indoleamine 2,3-dioxygenase protects engraftment of xenogeneic skin substitute. J Invest Dermatol **126,** 128, 2006.
37. Phillips, C.L., Combs, S.B., and Pinnell, S.R. Effects of ascorbic acid on proliferation and collagen synthesis in relation to the donor age of human dermal fibroblasts. J Invest Dermatol **103,** 228, 1994.

Address correspondence to:
Aziz Ghahary, PhD
University of British Columbia
Burn and Wound Healing Lab
4550-818 W 10th Avenue
Vancouver
BC V5M 1Z9
Canada

E-mail: aghahary@mail.ubc.ca

Received: May 12, 2014
Accepted: October 23, 2014
Online Publication Date: February 18, 2015